RESEARCH ARTICLE

Compact Empirical Model for Droplet Generation in a Lab-on-Chip Cytometry System

KAISER PÄRNAMETS [1], (Graduate Student Member, IEEE), **ANDRES UDAL** [2], (Member, IEEE),
ANTS KOEL [1], (Member, IEEE), **TAMÁS PARDY** [3], (Member, IEEE), **NAFISAT GYIMAH** [1],
AND TOOMAS RANG [1,3], (Senior Member, IEEE)

[1]Thomas Johann Seebeck Department of Electronics, Tallinn University of Technology, 19086 Tallinn, Estonia
[2]Department of Software Science, Tallinn University of Technology, 19086 Tallinn, Estonia
[3]Department of Chemistry and Biotechnology, Tallinn University of Technology, 19086 Tallinn, Estonia

Corresponding author: Kaiser Pärnamets (kaiser.parnamets@taltech.ee)

ABSTRACT This study describes the construction of a droplet generation speed compact empirical mathematical model for a flow-focusing microfluidic droplet generator. The application case is a portable, low-cost flow cytometry system for microbiological applications, with water droplet sizes of 50-70 micrometer range and droplet generation rates of 500-1500 per second. In this study, we demonstrate that for the design of reliable microfluidic systems, the availability of an empirical model of droplet generation is a mandatory precondition that cannot be achieved by time-consuming simulations based on detailed physical models. When introducing the concept of a compact empirical model, we refer to a mathematical model that considers general theoretical estimates and describes experimental behavioral trends with a minimal set of easily measurable parameters. By interpreting the experimental results for different water- and oil-phase flow rates, we constructed a minimal 3-parameter droplet generation rate model for every fixed water flow rate by relying on submodels of the water droplet diameter and effective ellipticity. As a result, we obtained a compact model with an estimated 5-10% accuracy for the planned typical application modes. The main novelties of this study are the demonstration of the applicability of the linear approximation model for droplet diameter suppression by the oil flow rate, introduction of an effective ellipticity parameter to describe the droplet form transformation from a bullet-like shape to a spherical shape, and introduction of a machine learning correction function that could be used to fine-tune the model during the real-time operation of the system.

INDEX TERMS Compact empirical model, droplet cytometry, droplet generation, flow-focusing junction, microfluidic chip.

I. INTRODUCTION

Bacterial threats have been a noticeable challenge of this century, and a delayed response due to the lack of field-testing options poses risks to human lives and can cause epidemics. Classical microbiological methods are relatively slow, while cytometric methods allow measuring the number and morphology of cells easily, reliably, and quickly. Droplet microfluidics, a new technology developed over the last dozen years, offers breakthrough solutions for creating low-cost, fully portable cytometers for field analysis of bacteria based on very small sample volumes and the possibility of seeking single-cell resolutions.

The present study discusses model-based design of portable cytometer devices based on the concepts of lab-on-a-chip [1], [2], [3], microfluidics [4], [5], and droplet cytometry [6], [7], [8], [9], [10]. Specifically, we describe the construction of an empirical mathematical model for the calculation of droplet generation rates and dimensions in the water-in-oil flow-focusing-type [11] droplet generation node of a lab-on-a-chip cytometer. This study was partly based on the digital twin model developed by our group [12].

Figure 1 illustrates the topicality trends of the considered research areas based on the publication statistics of the

The associate editor coordinating the review of this manuscript and approving it for publication was Kin Fong Lei [ID].

Clarivate Web of Science database [13]. As demonstrated in Figure 1, the concept of lab-on-a-chip has become popular since the beginning of the 21st century, and is presently showing a saturation trend. The overall area of droplet microfluidics became popular slightly later in years 2003-2004 and has demonstrated linear growth until the present time. The most vital concept is droplet cytometry, for which exponential growth with a doubling time of 4-5 years started approximately 12 years ago. An overall comparison of regions over the last decade demonstrated the approximate equality of Western Europe, North America, and the People's Republic of China (PRC) [13].
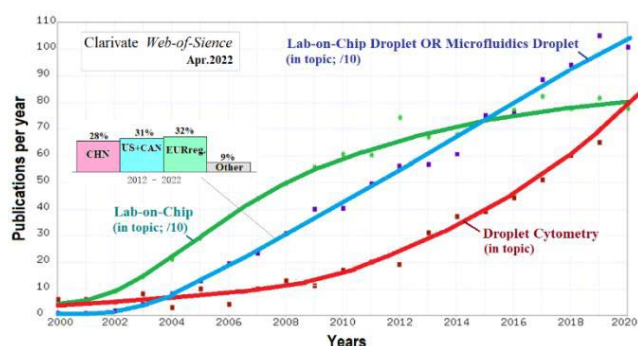
FIGURE 1. Research intensity trends on basis of Clarivate Web of Science publication statistics [13]. Dynamics of the most relevant subfields as Lab-on-Chip, droplet microfluidics and droplet cytometry is compared. Inlet compares contributions from People's Republic of China, North America and European region (incl. Turkey and Israel).

Model-based design has become a mandatory methodology for system design in various applications, including microfluidics [14], [15], [16], [17]. In the present use case, a model of the droplet generation node is required for the prediction of droplet generation parameters, such as generation rates and diameters, both during the cytometer construction and exploitation phases, to improve the control quality via model predictive control.

An important issue in the construction of a mathematical model for any object is the selection of a detailed physical or formal empirical approach [18], [19], [20], [21]. The physical approach can be time consuming for both the computer and developer but can yield reliable results for a wide range of operation conditions, provided that the physical mechanisms and relevant key parameter values are known and modelled correctly. In the case of droplet microfluidics, physical models rely on well-known equations and methods of computational fluid mechanics (CFD), which must be supplemented with less reliable multicomponent fluid flow methods [22], [23]. Thus, in addition to the high computational workload, the major problem of the physical approach is often the presence of non-measurable physical parameters and the hidden influence of numerical factors such as reduced spatial dimensionality and mesh step sizes. Although many authors have illustrated their studies with simulated droplet images, for example, [23], [24], [25], [26], several respected research groups, for example, [24], [27],

[28], [29], emphasize the unreliability of numerical physical modelling, particularly if the droplet size, generation rate, and monodispersity characteristics must all be reliably calculated simultaneously. Moreover, considering the three main droplet generation geometry types – co-axial, T-junction and flow-focused [27], [30], the third option, which is also analyzed in the present study, has been estimated most difficult for the point of view of accurate modelling [20], [30], [31]. Our simulation results with the COMSOL Multiphysics®5.6 Two-Phase Flow Level Set module [32], described below in the simulation section, confirm the unreliability claims regarding the detailed physical modelling approach. To illustrate the relevant difficulties, it is reasonable to point out that to overcome the aforementioned uncertainties and obtain a reliable practical tool for flow-focusing droplet generator design, a large-scale experimental study was recently conducted by the group of Boston University [24], [28]. In this study, a generalized flow-focusing structure with an orifice was described using six geometrical parameters: 25 orthogonal structure variants were manufactured using the Taguchi formal scheme, over 30 operation modes for each structure were tested, and a statistical empirical model was obtained to cover a reasonably wide range of droplet diameters and generation rates. In comparison with [24], [28], the present study discusses only one flow-focusing structure without nozzle (orifice) section but, on the other hand, the droplet geometry description includes also the ellipticity factor, droplet generation rates are of 2-3 times higher range and the formula-based analytic formulation having a better transparency and real-time adjustability is used.

In contrast to detailed physical models, the alternative empirical approach is characterized by a formal generalization of experimental data [20], [27], [30]. The empirical approach is usually less labor-intensive and often more accurate, but only for the parameter space covered by the experiments. In practice, the most useful real models are semi-empirical, which means that they combine theoretical principles with available experimental data. In droplet microfluidics, it is reasonable to build all droplet generation models based on the mass conservation principle for the dispersed phase (i.e., droplet fluid-like water), which allows a state connection between three main variables: droplet fluid flow rate, droplet diameter, and droplet generation rate [20], [21], [28], [31]. Some authors, who have investigated the formation of relatively large non-spherical droplets that fill all cross-sections of the generation channel, have added a fourth parameter, the droplet length, for example, [20], [21], [30]. In this study, we introduce an original approach using an effective ellipticity parameter that maintains droplet volume conservation and accounts for experimentally observed droplet shape changes from bullet-like shapes at low continuous-phase flow rates to spherical shapes at high continuous-phase flow rates.

When discussing the droplet diameter empirical models, many authors have used the ratio of dispersed and continuous phase flow rates Q_d/Q_c, for example, [21], [25], [26].

Our droplet image recording results, presented below in the experimental section, do not support the use of this ratio parameter, and demonstrate that for higher water flow values, a proportional oil flow increase is required to achieve a comparable diameter suppression effect.

An important characteristic for the practical applicability of mathematical models is their compactness. We recommend defining compactness based on the following features:1) the minimal number of adjustment parameters, 2) measurability of the adjustment parameters, 3) low computational workload, and 4) transparency of the set of equations [33]. The concept of a compact model is widely used in the field of electronic and semiconductor microchip design [34] for two main reasons: lowering the computational workload and operation with measurable parameters. In droplet microfluidics, the need for compact models has not yet been explicitly recognized and only a few studies have used this term. However these studies have focused solely on estimating the length of droplets based on the ratio of dispersed and continuous phase flowrates [35], [36], [37], [38]. At the same time, nearly 1000 publications (see Figure 1) contain some approximate formulas for the calculation of droplet sizes or generation rates that may be interpreted as compact models for solving some subproblems of droplet microfluidic system design tasks.

An important question in droplet generation model construction is the description of the droplet diameter suppression effect owing to continuous phase (oil) flow. The majority of published results and models, for example, [25], [26], [39], predict a less-than-proportional diameter suppressing effect owing to the increasing continuous phase flow rate Q_c. Few studies support either a proportional decrease in diameter, for example, [31], or a stronger than proportional increase [26]. The present experimental study confirmed the applicability of the linear approximation of the dependence of the water droplet diameter on the oil flow rate. Thus, a linear droplet diameter model may be offered that uses only one proportionality factor for a fixed water flow rate and given droplet generation channel width. If completed with two parameters for the description of effective ellipticity changes, a compact 3-parameter model for the calculation of droplet diameters, ellipticities, and generation rate dependencies on the oil flow rate may be constructed.

In recent years, there has been an urgent need to accelerate and simplify the development of microfluidic droplet generators with desired output parameters via automatization and the application of machine learning methods [24], [40], [41]. To realize these goals via empirical statistical modelling by applying artificial neural networks, large-scale experimental testing [24], [28] or sophisticated computer vision methods for additional droplet data collection [40] have been proposed. In this study, a much narrower task scope was considered and only the desired droplet parameters were obtained by adjusting the water and oil flow rates for a fixed microfluidic chip. However, formula-based transparent presentation of mathematical models offers much better possibilities for

solving system optimization and real-time model adjustment (i.e., machine learning) tasks. Although the modification of neural-network-based statistical models [24], [40] requires significant effort and time for the collection of additional data and retraining (transfer learning), the empirical model considered here, in the form of mathematical formulas with adjustable coefficients, offers possibilities for the realization of real-time model adjustment and a cytometer system with an extremely simple feedback loop containing an elementary optical sensor.

The remainder of this paper is organized as follows. In Section 2, the microfluidic chip and the measurement setup are described. In Section 3, a short summary of the detailed numerical simulation results and a discussion of the problems that occurred are presented. Section 4 summarizes the experimental results for the different water and oil flow rates. In section 5, the construction principles, formulas, and fitting results of the compact mathematical model are presented. Section 6 discusses the scope of the application of the proposed model. Section 7 presents the main results of the study.

II. DESCRIPTION OF DROPLET GENERATION CHIP AND MEASUREMENT SETUP

Microfluidic droplets were generated inside a polydimethylsiloxane (PDMS) chip, as shown in Figure 2. The full thickness of the PDMS chip was 5 mm, and it had a microfluidic channel structure with a depth of 100 μm on one surface (Figure 2a), which was covered by a 1 mm thick glass plate (microscope slide plate). From the three main droplet generation geometries, the T-junction, co-flow, and flow-focusing junction [11], the last geometry variant, where water flows with biological agents, is cut into droplets by a continuous oil flow entering the junction area from the two opposite sides (Figure 2a and 2c). Thus, water droplets were formed in the junction area and in the generation channel with cross-sectional dimensions of 84 μm width and 100 μm height. An overview of the droplet generation unit with the inlet and outlet tubes is shown in Figure 2b. Deionized water was used as the dispersed phase (droplets). For the continuous phase, Sigma-Aldrich 330779 mineral oil [42] with a 2% surfactant [43] was used. The water and oil flow rates were maintained using syringe pumps and software manufactured by SpinSplit [44]. The lighting of the droplet generation junction area was realized from the PDMS side of the chip using a white LED group consisting of two LEDs with cold-color temperatures and two LEDs with warm-color temperatures. Photorecording was accomplished using a Basler Ace acA640-750um camera in a reduced resolution mode that allowed a frame rate of up to 3300 per second at an exposure time of 100 μs. Thus, as the experiment shows, a droplet per second (*dps*) generation rate of up to 1600 s^{-1} can be directly determined from the sequence of the recorded images. Additionally, *dps* values up to 2300 s^{-1} can be extrapolated based on the droplet separation distances (see Figure 7).
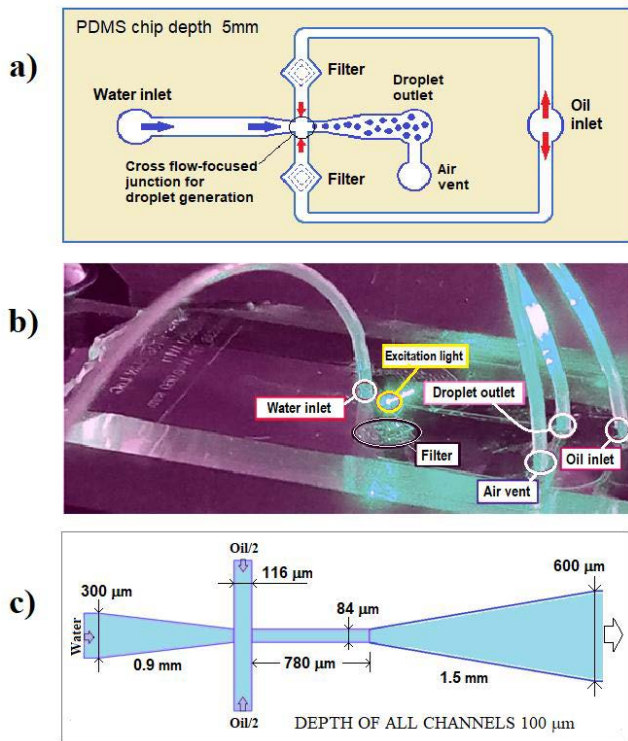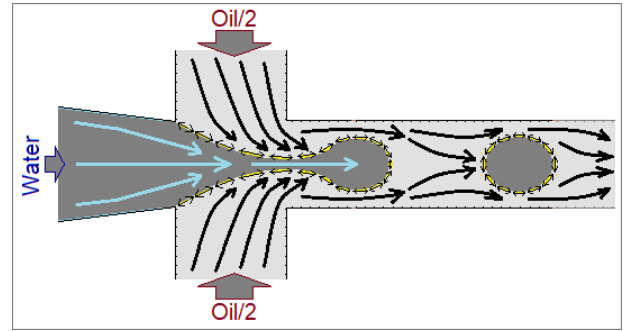
FIGURE 2. Description of the droplet generation PDMS chip: a) Water droplets generation scheme in the flow focusing cross-junction; b) Photo of the setup with inlet and outlet tubes and photorecording area; c) Exact dimensions of channels near the flow focusing junction.

FIGURE 3. Illustration of competing processes of water droplets generation in a flow-focusing cross-junction. The incoming water stream tries to maintain the minimum surface area due to the surface tension forces but is divided into droplets by the "oil pliers" acting from both sides. After that the surface tension helps to maintain the size of droplets already formed, provided that the adjacent droplets are at a sufficient distance. At that all flow speeds are decelerated near the walls because of the wall friction effect.

III. INTRODUCTORY SIMULATIONS OF UNDERLYING PHYSICS

In general, the prerequisite for the construction of a compact model may be the availability of experimental data or, as an alternative, the availability of a sufficiently reliable detailed physical model with necessary input data. In the case of flow-focused droplet generation junctions, the choice of the detailed physical approach can be complicated by the complex nature of the task, that is, the need for accurate modelling of the balance of competing processes of separation and encapsulation of droplets. Another serious problem is the high computational time required for realistic three-dimensional calculations. Therefore, all affordable two-dimensional calculations, even if the parameters of the physical processes are correctly estimated, can only serve as predictions that need to be confirmed by real experiments. Figure 3 shows the critical competing processes that must be accurately modelled in a flow-focused junction. Figure 3 emphasizes the importance of accurately modelling the surface tension forces, viscosities of both liquids, wall friction effects, channel dimensions, and other factors to obtain a realistic picture of both the liquid flow and droplet formation processes.

To test the possibility of using detailed physical modelling to formulate the basis of the droplet generation model, we performed several numerical simulation series using the COMSOL Multiphysics®5.6 Two-Phase Flow Level Set module [32] in the traditional two-dimensional (2D) axisymmetric approximation of geometry [11]. It is important to emphasize that the crucial point for the accuracy of all modelling approaches is the correct handling of water volumes in the task specification. Oil can be considered an auxiliary substance that splits the incoming water stream and suppresses the diameters of the formed water droplets. Because in the 2D-simulation the droplets are cylindrical rather than spherical, the first question in the specification of the 2D-simulation task is to correctly select the effective size of the simulated structure towards the third dimension. Considering the realistic situation of the 3D-experiment (at high oil flow rates), it can be assumed that the droplets are spheres with a volume

$$V_{exp} = \frac{\pi}{6} D_{exp}^3 \qquad (1)$$

where D_{exp} is the droplet diameter used in this experiment. In the 2D simulations, the volume of the droplet was defined using the cylinder formula

$$V_{sim} = \pi \cdot \left(\frac{D_{sim}}{2}\right)^2 \cdot H_{eff} \qquad (2)$$

where H_{eff} is the introduced effective size of the structure towards the third dimension (see Figure 4).

The diameter and volume of the droplets must be equal to match the water volume counts in the experiments and simulations. Figure 4 shows the methodology for achieving the aforementioned water volume balance conditions when the auxiliary parameter H_{eff} of the 2D-simulation is specified as follows:

$$H_{eff} = \frac{2}{3} D_{exp}. \qquad (3)$$

Specifically, if the actual expected droplet diameter is 60 μm (in the 84 μm channel), then a reasonable measure for the structure depth in 2D-simulations should be 40 μm.

Figure 5 summarizes the main results of the COMSOL 2D-simulations with the Two-Phase Flow Level
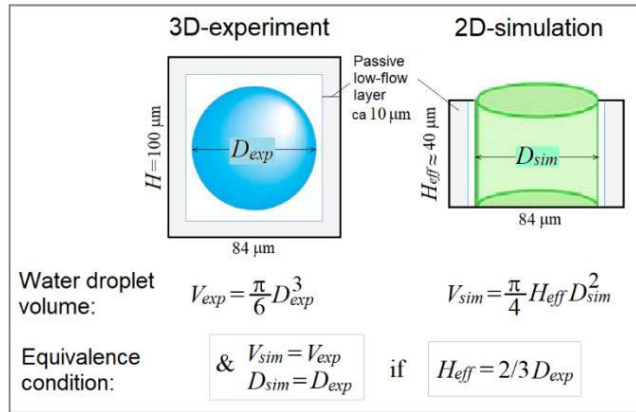
FIGURE 4. Graphical representation of droplet volumes in real life 3D-experiment and in simplified 2D-simulation.

Set module [32] for the droplet generation area described in Figure 2c. For the first adjustment parameter, the effective depth of the structure in the third dimension was specified as 40 μm based on the considerations explained above. For the second essential adjustment parameter, the surface tension coefficient values of $\sigma = 40 \div 50$mN/m were used to avoid the jetting effect and ensure the acceptable stability of the formed droplets. High surface tension values in a similar range have been recommended for water-to-mineral oil interfaces, for example, in [45] and [46]. Next, in presented simulations the "no-slip" sub model of high friction walls was used. Other models, such as the Navier slip model with several additional adjustment parameters, did not cause essential changes.

For the main computational parameters, that is, the spatial mesh size, the two standard cases of "Fine" with 9536 finite elements and "Finer" with 36626 elements were compared. The computational times for the relatively short 20 ms process calculation ranged from 2 h to 14 h on a powerful desktop 16-core Intel i9-computer.

The main results of the COMSOL simulations are shown in Figure 5. The results demonstrate the difficulty of achieving stable droplet diameters and droplet generation rates. When the spatial mesh size was increased to a very high number of final elements, instead of the expected stabilization of the main output parameters, the chaotic behavior of the results demonstrated a remarkable increase, and the definition of certain values of droplet diameters and droplet generation rates became impossible. This emerging instability and uncertainty may be caused by the difficulty of the task, as shown in Figure 3. In summary, detailed physics-based numerical simulations provide supporting explanations for the underlying physical processes. However, the expected results for building a compact model for droplet generation have not been obtained.

IV. SUMMARY OF EXPERIMENTAL RESULTS
For the actual microfluidic chip, the expected droplet generation rates were in the range of 500-1500 per second, with

droplet diameters of 50-70 micrometer range. Based on these design goals, three test series with constant water flow rates $Q_w = 4, 8$, and 12μL/min and varying oil flow rates from value $Q_{oil} = 2Q_w$ to value $Q_{oil} = 60 \div 88\mu$L/min in steps of 4 μL/min were performed. The selection of droplet images recorded in the beginning section of the 84 μm generation channel is presented in Figure 6. The results in Figure 6 show that at low oil flow rates, the droplets resemble bullets (modelled by the effective ellipsoids below in this study). With an increase in the oil flow rate, the droplets begin to resemble spheres. Simultaneously, the diameter can be suppressed by increasing the oil flow rate. The increasing blurring of droplet fronts and backs at higher droplet formation rates is due to camera exposure settings (100 μs).

An overall summary of the experimental results, including the directly recorded and extrapolated *dps* values from the droplet separation distances, is shown in Figure 7. The experimental diameters of droplet D were obtained by carefully comparing the droplet lateral sizes with a channel width of 84 μm and smoothing the dependencies with the neighboring points. Thus, the estimated accuracy of the diameters was of the order of ± 2 μm. The effective ellipticity numbers, E (approximate ratio of the vertical and horizontal sizes of the droplets in the images), were estimated from the principle of equivalent volumes of the imaginary ellipsoidal and real bullet-like droplets. Additionally, minor smoothing of the experimental diameter and effective ellipticity values was performed to ensure correlation with the real water flow rates.

Owing to the camera frame rate limit, the high droplet rate values over *dps* > 1600 s^{-1} were difficult to define from video recordings but were extrapolated on the basis of the observed decrease in droplet distances (see inlet in the upper part of Figure 7). Regarding this extrapolation, it should be mentioned that because of the increasing influence of the friction of the channel walls at higher Q_{oil} rates, the size of the effective high-flow-speed center area of the channel may be smaller at high Q_{oil} values; thus, the extrapolated *dps* numbers may be underestimated.

V. CONSTRUCTION OF THE COMPACT EMPIRICAL MODEL
In the present microfluidic system design, the main purpose of developing a compact droplet generation model is to obtain a tool for estimating the droplet generation rate *dps*. The latter depends directly on the droplet volume estimation by the sub-models for the droplet size parameters, such as the diameter D and effective ellipticity E, if the water flow rate Q_w is given. The oil flow rate Q_{oil} can be interpreted as an auxiliary factor that suppresses D compact model and can be constructed based on the following approximations:

1) For droplet generation rate *dps*, recalculation from a single ellipsoidal droplet volume formula $V = E (\pi/6) D^3$ can be applied if the diameter and ellipticity are estimated with reasonable accuracy.

2) Initially, it is reasonable to consider all three water flow rate values $Q_{w,i}$ separately. The final result for any Q_w value
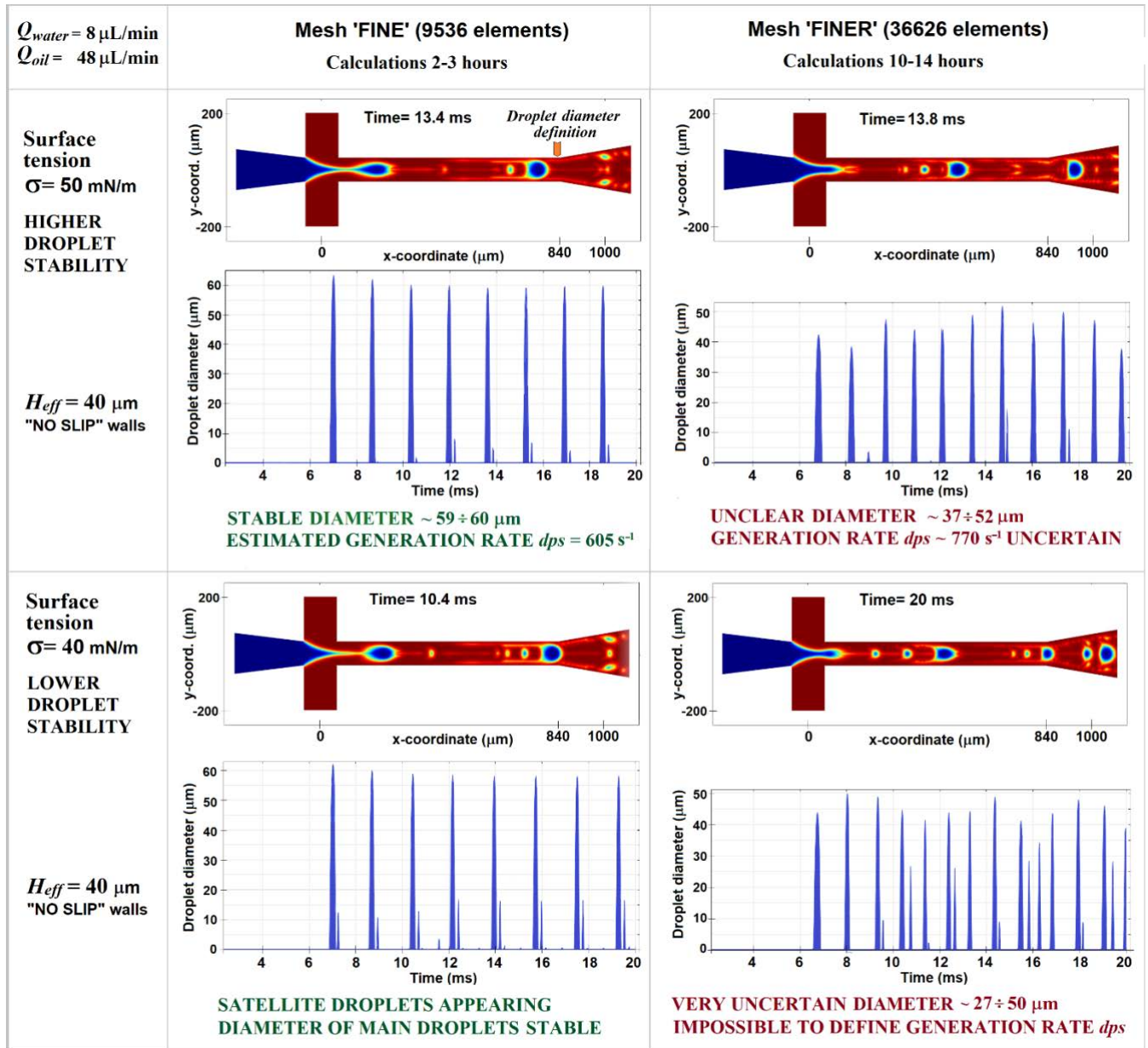
FIGURE 5. Illustration of appearance of droplet generation instabilities in detailed physical 2D-simulations with COMSOL 5.6 [32].

can be interpolated based on three separate results for dps_i, D_i, and E_i.

3) Relying on Figure 7 and seeking the principle of minimal complexity, for diameter dependence on oil flow rate $D(Q_{oil})$ the simplest single-parameter linear dependences may be applied; for the zero-oil origin point, the actual channel width value of 84 μm can be used as a common constant. The changes in dps in the 10% range were acceptable for an approximate adjustable model.

4) For E, the decreasing exponent law can be applied with a final level at high oil rate values close to one, which corresponds to the spherical limit form.

5) For machine learning readiness one real-time adjustable correction function $C_{ML}(Q_w, Q_{oil})$ may be added.

Considering the principles described above, the following set of mathematical equations can be proposed for the compact model (for every water flow rate value $Q_{w,i}, i = 1, 2, 3$):

$$dps_i = \left(557 \text{ s}^{-1}\right)\left(\frac{Q_{w,i}}{6 \text{ }\mu\text{L/min}}\right)\left(\frac{1}{E_i}\right)\left(\frac{70 \text{ }\mu\text{m}}{D_i}\right)^3 \quad (4)$$

$$D_i = (84 \text{ }\mu\text{m})\left(1 - \frac{Q_{oil}}{Q_{D,i}}\right) \quad (5)$$

$$E_i = 1 + (E_{8,i} - 1)\exp(-\frac{(Q_{oil} - 8 \text{ }\mu\text{L/min})}{Q_{E,i}}) \quad (6)$$

where, following the goal of minimizing the number of adjustable parameters, only three fitting parameters, $E_{8,i}, Q_{E,i}, Q_{D,i}$ were introduced for each of the tested water

TABLE 1. Best fit compact model parameter values for considered 3 water flow rates.

Water rate series index i	Water flow rate $Q_{w,i}$, µL/min	Ellipticity $E_{8,i}$ at low oil rate $Q_{oil}=$ 8 µL/min	Exponential decay parameter of ellipticity $Q_{E,i}$, µL/min	Linear decay parameter of droplet diameter $Q_{D,i}$, µL/min
1	4	2.6	9.9	157
2	8	3.6	10.4	196
3	12	4.15	12.4	248
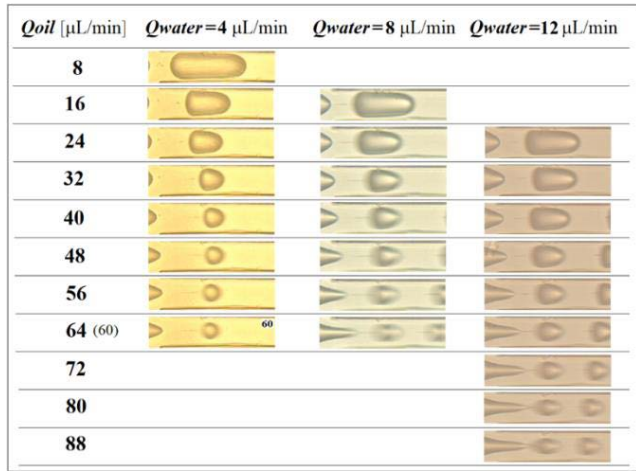
FIGURE 6. Summary of droplet photos for different water and oil flow rate values in beginning section of 84 µm generation channel. Different coloring is caused by slightly changed LED lighting between experimental series. The transform from bullet-like shapes at low oil flow rates to spherical shapes at high oil flow rates may be observed. Increasing blur of photos at high oil flow rates is caused by camera shutter time 100 µs.

flow rate values: $Q_{w,1} = 4$ µL/min $Q_{w,2} = 8$ µL/min, and $Q_{w,3} = 12$ µL/min (see Figure 6).

In systems (4)–(6), equation (4) is constructed to transform the value of the water flow rate to the number of droplets per second, considering the lateral diameter of droplets D_i and the effective ellipticity E_i as key parameters for the calculation of a single droplet volume. Equation (5) postulates the simplest linear decrease law for droplet diameters by introducing only one adjustable parameter $Q_{D,i}$ for every water rate, and using an actual channel width of 84 µm as a fixed constant for the low oil flow limit. Equation (6) approximates the exponential decrease in effective ellipticity from the initial high value at $Q_{oil} = 8$ µL/min to the final unit value using two adjustment parameters: $E_{8,i}$ and $Q_{E,i}$.

For the general case of any water flow rate between 4 and 12 µL/min, the simplest reliable piecewise linear approximation may be offered, considering that higher-order approximations such as parabolic approximations may distort the monotony of the dependences. In addition, an advanced feature of machine learning readiness may be included in the real-time empirical adjustment function $C_{ML}(Q_w, Q_{oil})$ for dps. In the minimal model formulation, the droplet size parameters may be excluded from the real-time adjustment because they droplet size parameters are difficult to measure during real-time operation.

Thus, the piecewise linear interpolation-based generalization of the droplet generation rate calculation for any water rate value can be performed using equations (7) and (8) given below.

The mathematical formulation of the linear approximation with machine learning adjustment for the first interval $Q_{w,1} \leq Q_w \leq Q_{w,2}$ can be written as

$$dps = C_{ML}(Q_w, Q_{oil})(A_{21} dps(Q_{w,1}) + B_{21} dps(Q_{w,2})),$$
$$A_{21} = \frac{Q_{w,2} - Q_w}{Q_{w,2} - Q_{w,1}}, B_{21} = 1 - A_{21} \tag{7}$$

and for the second interval $Q_{w,2} \leq Q_w \leq Q_{w,3}$ as

$$dps = C_{ML}(Q_w, Q_{oil})(A_{32} dps(Q_{w,2}) + B_{32} dps(Q_{w,3})),$$
$$A_{32} = \frac{Q_{w,3} - Q_w}{Q_{w,3} - Q_{w,2}}, B_{32} = 1 - A_{32}. \tag{8}$$

The fitting of the three parameters of models (4)–(6) to determine the best agreement between the model and experimental points in Figure 7 was performed by separately minimizing the root-mean-square (RMS) difference between the experiment and simulation for the three water rate values. The weight scalers for the three main output parameters, dps, D, E were 20 s^{-1}, 2 µm, and 0.1, respectively. In addition, the weights of the low oil rate endpoints for the high water rate curves $Q_{w,2}$, $Q_{w,3}$ were increased to obtain a reasonable balance with the low water $Q_{w,1}$ curve. The overall results of the fitting are shown in Figure 8. The values obtained for the model coefficients are listed in Table 1.

VI. DISCUSSION AND APPLICATION AREA

The definition of the application area is an important issue in empirical models. The general principle is that the reliability of the results can only be assumed in the range of parameter values covered by the experimental results. The application area of the proposed compact empirical model is illustrated in Figure 9. In addition, we compared our experimental results with existing droplet length estimation models and found that existing models are also suitable for our microfluidic setup after some modifications to microfluidic chip-dependent parameters [35], [36], [37], [38]. It is important to emphasize that previous studies have solely focused on estimating the length of droplets.

As shown in Figure 8, the droplet rate calculation accuracy of the proposed compact model remained in the range of 20% when considering the all-parameter area. However, it is
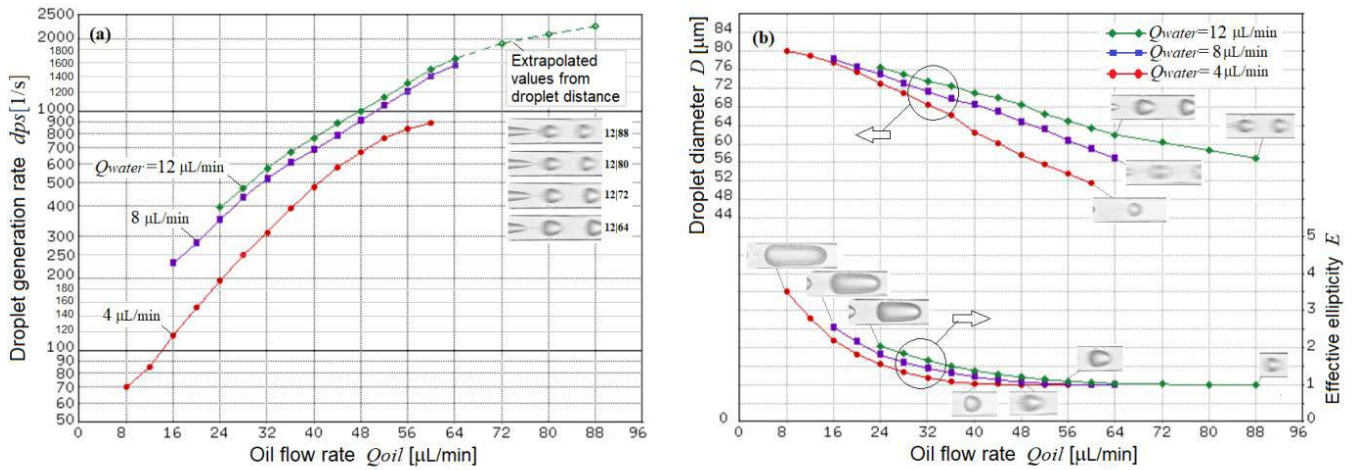
FIGURE 7. Overall summary of experimental results for droplet generation rates (a) and droplet diameters and ellipticities (b).
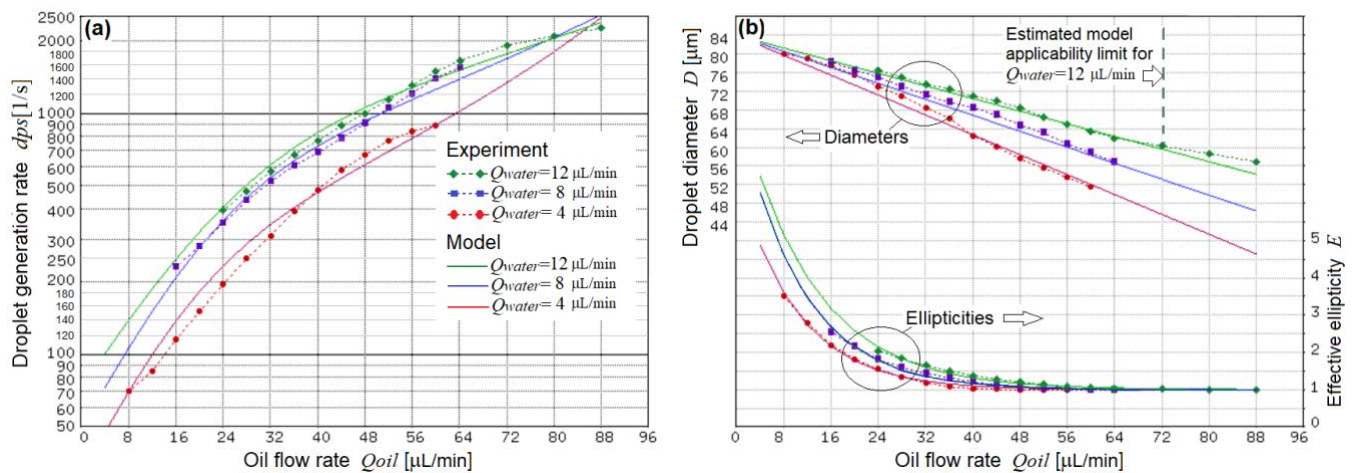

FIGURE 8. Summary of fitting results of compact empirical model (4)-(6) against experimental points for 3 water flow rate values: droplet generation rates (a); droplet diameters and ellipticities (b). Model results are presented by solid lines, experimental points by marker symbols and dotted lines.
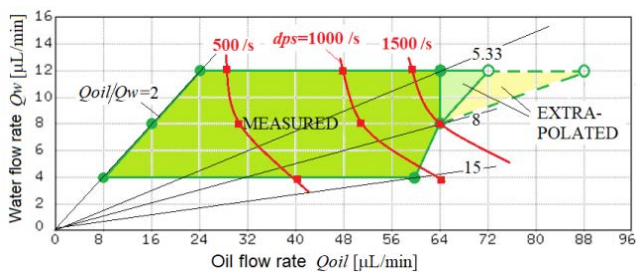

FIGURE 9. Illustration of application area of compact empirical model on the plane of water and oil flow rates.

important to emphasize that the trends of changes due to water and oil flow rate changes were modelled correctly. Additionally, for the central region of the planned operation around dps = 500-1500 s^{-1} the accuracy is much better and is already in the 5-10% range. Moreover, this number can be improved by machine-learning adjustments during real operations if the droplet generation rates are measured using optical measurements.

The reason for the moderate accuracy of the proposed simple 3-parameter model is the simplicity of modelling the droplet diameter using the simplest 1-parameter linear dependence. Since the droplet formation rate depends on the droplet diameter according to the cubic law, small differences in diameters of about 3% were increased to 10% when the formation rates were taken into account. It is possible to introduce a sub-model of a more precise diameter; however, the accompanying increase in the number of model parameters may require additional complex measurements.

From a technical viewpoint, it seems more reasonable to use a simpler model with the possibility of real-time adjustment.

VII. CONCLUSION
Compact models are a well-established approach in electronics and microelectronics but are not yet sufficiently appreciated in the relatively young field of droplet microfluidics. Although for design of any technical system, like droplet cytometry portable apparatus in the present use case, the availability of compact models for all subsystems is a highly

desirable precondition for the successful design of the system as well for later exploitation of the system. In addition, as demonstrated in the present study, the alternative approach of detailed physical modelling may not yield usable results in the case of the droplet generation task of microfluidics, where the competing balances of different physical mechanisms must be accurately modelled.

The original new results presented in the present study may be summarized as follows:

1) For the first time, a compact empirical model of droplet generation speed has been developed.

2) The applicability of the linear approximation of the dependence of the droplet diameter on the oil flow rate for the actual flow-focusing microfluidic water droplet generator task (droplet sizes in the 50-70 micrometer range and generation rates in the 500-1500 per second range) was demonstrated.

3) The concept of effective ellipticity was introduced to describe a unified model for the change of droplet geometry from a bullet-like to a spherical shape.

4) The methodology for the construction of a minimized compact 3-parameter droplet generation rate model with 5-10% accuracy for the calculation of the oil flow rate dependence at fixed water flow rates for the desired operation region was described.

5) A machine learning extension to the basic model for further adjustment using real-time measurement results was proposed.

6) The droplet-volume-based equivalence condition to make 2D-simulations comparable to the real 3D experimental geometry is discussed.

REFERENCES

[1] P. S. Dittrich and A. Manz, "Lab-on-a-chip: Microfluidics in drug discovery," *Nature Rev. Drug Discovery*, vol. 5, no. 3, pp. 210–218, Mar. 2006, doi: 10.1038/nrd1985.

[2] J.-Y. Yoon and B. Kim, "Lab-on-a-chip pathogen sensors for food safety," *Sensors*, vol. 12, no. 8, pp. 10713–10741, Aug. 2012, doi: 10.3390/S120810713.

[3] H. Craighead, "Future lab-on-a-chip technologies for interrogating individual molecules," *Nature*, vol. 442, no. 7101, pp. 387–393, Jul. 2006. [Online]. Available: https://www.nature.com/articles/nature05061, doi: 10.1038/nature05061.

[4] S. Haeberle and R. Zengerle, "Microfluidic platforms for lab-on-a-chip applications," *Lab Chip*, vol. 7, no. 9, pp. 1094–1110, Apr. 2007, doi: 10.1039/B706364B.

[5] R. Pol, F. Céspedes, D. Gabriel, and M. Baeza, "Microfluidic lab-on-a-chip platforms for environmental monitoring," *Trends Anal. Chem.*, vol. 95, pp. 62–68, Oct. 2017, doi: 10.1016/J.TRAC.2017.08.001.

[6] M. Grafton, L. M. Reece, P. P. Irazoqui, B. Jung, H. D. Summers, R. Bashir, and J. F. Leary, "Design of a multi-stage microfluidics system for high-speed flow cytometry and closed system cell sorting for cytomics," *Proc. SPIE*, vol. 6859, pp. 187–198, Feb. 2008, doi: 10.1117/12.764037.

[7] J. Fattaccioli, J. Baudry, J.-D. Émerard, E. Bertrand, C. Goubault, N. Henry, and J. Bibette, "Size and fluorescence measurements of individual droplets by flow cytometry," *Soft Matter*, vol. 5, no. 11, pp. 2232–2238, May 2009, doi: 10.1039/B814954B.

[8] M. Li, H. Liu, S. Zhuang, and K. Goda, "Droplet flow cytometry for single-cell analysis," *RSC Adv.*, vol. 11, no. 34, pp. 20944–20960, Jun. 2021, doi: 10.1039/D1RA02636D.

[9] M. Vitelli, H. Budman, M. Pritzker, and M. Tamer, "Applications of flow cytometry sorting in the pharmaceutical industry: A review," *Biotechnol. Prog.*, vol. 37, no. 4, p. 17, Apr. 2021, doi: 10.1002/BTPR.3146.

[10] H. Yang, Y. Wei, B. Fan, L. Liu, T. Zhang, D. Chen, J. Wang, and J. Chen, "A droplet-based microfluidic flow cytometry enabling absolute quantification of single-cell proteins leveraging constriction channel," *Microfluidics Nanofluidics*, vol. 25, no. 4, pp. 1–11, Apr. 2021, doi: 10.1007/S10404-021-02427-W.

[11] W. Han and X. Chen, "A review on microdroplet generation in microfluidics," *J. Brazilian Soc. Mech. Sci. Eng.*, vol. 43, no. 5, pp. 1–12, May 2021, doi: 10.1007/S40430-021-02971-0.

[12] N. Gyimah, O. Scheler, T. Rang, and T. Pardy, "Digital twin for controlled generation of water-in-oil microdroplets with required size," in *Proc. 23rd Int. Conf. Thermal, Mech. Multi-Phys. Simulation Exp. Microelectron. Microsyst.*, Apr. 2022, pp. 1–7, doi: 10.1109/EuroSimE54907.2022.9758876.

[13] Web of Science. (2022). *The Clarivate Web of Science™ Publisher-Independent Global Citation Database*. Accessed: Apr. 24, 2022. [Online]. Available: https://clarivate.com/webofsciencegroup/solutions/web-of-science/

[14] H. Hjalmarsson, M. Gevers, and F. De Bruyne, "For model-based control design, closed-loop identification gives better performance," *Automatica*, vol. 32, no. 12, pp. 1659–1673, Dec. 1996, doi: 10.1016/S0005-1098(96)80003-3.

[15] J. C. Jensen, D. H. Chang, and E. A. Lee, "A model-based design methodology for cyber-physical systems," in *Proc. 7th Int. Wireless Commun. Mobile Comput. Conf. (IWCMC)*, Jul. 2011, pp. 1666–1671, doi: 10.1109/IWCMC.2011.5982785.

[16] C. K. Harnett, J. Templeton, K. A. Dunphy-Guzman, Y. M. Senousy, and M. P. Kanouff, "Model based design of a microfluidic mixer driven by induced charge electroosmosis," *Lab Chip*, vol. 8, no. 4, pp. 565–572, Mar. 2008, doi: 10.1039/B717416K.

[17] A. Savran and G. Kahraman, "A fuzzy model based adaptive PID controller design for nonlinear and uncertain processes," *ISA Trans.*, vol. 53, no. 2, pp. 280–288, Mar. 2014, doi: 10.1016/J.ISATRA.2013.09.020.

[18] J. R. Thompson, *Empirical Model Building: Data, Models, and Reality*, 2nd ed. Hoboken, NJ, USA: Hoboken, NJ, USA: Wiley, 2011.

[19] P. A. Fritzson, *Introduction to Modeling and Simulation of Technical and Physical Systems With Modelica*. Hoboken, NJ, USA: Wiley, 2011.

[20] X. Chen, T. Glawdel, N. Cui, and C. L. Ren, "Model of droplet generation in flow focusing generators operating in the squeezing regime," *Microfluid. Nanofluidics*, vol. 18, nos. 5–6, pp. 1341–1353, May 2015, doi: 10.1007/s10404-014-1533-5.

[21] A. Biral, D. Zordan, and A. Zanella, "Modeling, simulation and experimentation of droplet-based microfluidic networks," *IEEE Trans. Mol., Biol. Multi-Scale Commun.*, vol. 1, no. 2, pp. 122–134, Jun. 2015, doi: 10.1109/TMBMC.2015.2500569.

[22] M. Wörner, "Numerical modeling of multiphase flows in microfluidics and micro process engineering: A review of methods and applications," *Microfluidics Nanofluidics*, vol. 12, no. 6, pp. 841–886, Mar. 2012, doi: 10.1007/S10404-012-0940-8.

[23] J. Kim, "Phase-field models for multi-component fluid flows," *Commun. Comput. Phys.*, vol. 12, no. 3, pp. 613–661, Sep. 2012, doi: 10.4208/CICP.301110.040811A.

[24] A. Lashkaripour, C. Rodriguez, L. Ortiz, and D. Densmore, "Performance tuning of microfluidic flow-focusing droplet generators," *Lab Chip*, vol. 19, no. 6, pp. 1041–1053, Mar. 2019, doi: 10.1039/C8LC01253A.

[25] M. Rahimi, S. Yazdanparast, and P. Rezai, "Parametric study of droplet size in an axisymmetric flow-focusing capillary device," *Chin. J. Chem. Eng.*, vol. 28, no. 4, pp. 1016–1022, Apr. 2020, doi: 10.1016/J.CJCHE.2019.12.026.

[26] A. Khater, M. Mohammadi, A. Mohamad, and A. S. Nezhad, "Dynamics of temperature-actuated droplets within microfluidics," *Sci. Rep.*, vol. 9, no. 1, pp. 1–11, Mar. 2019, doi: 10.1038/s41598-019-40069-9.

[27] S. L. Anna, "Droplets and bubbles in microfluidic devices," *Annu. Rev. Fluid Mech.*, vol. 48, no. 1, pp. 285–309, Jan. 2016, doi: 10.1146/ANNUREV-FLUID-122414-034425.

[28] A. Lashkaripour, C. Rodriguez, N. Mehdipour, R. Mardian, D. McIntyre, L. Ortiz, J. Campbell, and D. Densmore, "Machine learning enables design automation of microfluidic flow-focusing droplet generation," *Nature Commun.*, vol. 12, no. 1, pp. 1–14, Jan. 2021, doi: 10.1038/s41467-020-20284-z.

[29] A. Grimmer, M. Hamidović, W. Haselmayr, and R. Wille, "Advanced simulation of droplet microfluidics," *ACM J. Emerg. Technol. Comput. Syst.*, vol. 15, no. 3, pp. 1–16, Jul. 2019, doi: 10.1145/3313867.

[30] C. N. Baroud, F. Gallaire, and R. Dangla, "Dynamics of microfluidic droplets," *Lab Chip*, vol. 10, no. 16, pp. 2032–2045, Aug. 2010, doi: 10.1039/C001191F.

[31] W. Lee, L. M. Walker, and S. L. Anna, "Role of geometry and fluid properties in droplet and thread formation processes in planar flow focusing," *Phys. Fluids*, vol. 21, no. 3, Mar. 2009, Art. no. 032103, doi: 10.1063/1.3081407.

[32] *COMSOL Multiphysics 5.6, Laminar Flow and Two-Phase Flow, Level Set Modules. Two-Phase Flow Modeling Guidelines.* Accessed: May 3, 2022. [Online]. Available: https://www.comsol.com/support/knowledgebase/1239

[33] A. Udal, M. Jurise, J. Kaugerand, and R. Sell, "COMSPECT: A compact model of green vegetation reflectance spectra in the 400–900 nm wavelength range," *Proc. Estonian Acad. Sci.*, vol. 69, no. 4, pp. 277–286, 2022.

[34] G. Gildenblat, *Compact Modeling: Principles, Techniques and Applications.* Amsterdam, The Netherlands: Springer, 2010, doi: 10.1007/978-90-481-8614-3.

[35] A. S. Bedekar, Y. Wang, S. Krishnamoorthy, S. S. Siddhaye, and S. Sundaram, "System-level simulation of flow-induced dispersion in lab-on-a-chip systems," *IEEE Trans. Comput. Design Integr. Circuits Syst.*, vol. 25, no. 2, pp. 294–303, Feb. 2006, doi: 10.1109/TCAD.2005.858354.

[36] F. Lapierre, N. Wu, and Y. Zhu, "Influence of flow rate on the droplet generation process in a microfluidic chip," *Proc. SPIE*, vol. 8204, p. 8, Dec. 2011, doi: 10.1117/12.903271.

[37] F. Ender, M. Németh, P. Pálovics, A. Drozdy, and A. Poppe, "Thermal compact modeling approach of droplet microreactor based lab-on-a-chip devices," *Microelectron. J.*, vol. 45, no. 12, pp. 1786–1794, Dec. 2014, doi: 10.1016/J.MEJO.2014.07.005.

[38] A. Bonament, M. Madec, and C. Lallement, "Compact modeling of reaction-diffusion-advection mechanisms for the virtual prototyping of lab-on-chip," in *Proc. IEEE Int. Symp. Circuits Syst. (ISCAS)*, May 2021, pp. 1–5, doi: 10.1109/ISCAS51556.2021.9401396.

[39] K. I. Belousov, N. A. Filatov, I. V. Kukhtevich, V. Kantsler, A. A. Evstrapov, and A. S. Bukatin, "An asymmetric flow-focusing droplet generator promotes rapid mixing of reagents," *Sci. Rep.*, vol. 11, no. 1, pp. 1–10, Apr. 2021, doi: 10.1038/s41598-021-88174-y.

[40] A. E. Siemenn, E. Shaulsky, M. Beveridge, T. Buonassisi, S. M. Hashmi, and I. Drori, "A machine learning and computer vision approach to rapidly optimize multiscale droplet generation," *ACS Appl. Mater. Interfaces*, vol. 14, no. 3, pp. 4668–4679, Jan. 2022, doi: 10.1021/ACSAMI.1C19276.

[41] S. Srikanth, S. K. Dubey, A. Javed, and S. Goel, "Droplet based microfluidics integrated with machine learning," *Sens. Actuators A, Phys.*, vol. 332, Dec. 2021, Art. no. 113096, doi: 10.1016/J.SNA.2021.113096.

[42] *Sigma-Aldrich Mineral Oil. Sigma-Adrich Mineral Oil 330779-1L Data Page.* Accessed: May 3, 2022. [Online]. Available: https://www.sigmaaldrich.com/EE/en/product/sial/330779

[43] *Sigma-Aldrich Surfactant. Sigma-Adrich Span 80 (Code 840123100) Data Page.* Accessed: May 3, 2022. [Online]. Available: https://www.sigmaaldrich.com/EE/en/product/mm/840123

[44] SpinSplit. *Lab Equipment for Academic Research.* Accessed: May 3, 2022. [Online]. Available: https://spinsplit.com/spincube/

[45] W.-L. Ong, J. Hua, B. Zhang, T.-Y. Teo, J. Zhuo, N.-T. Nguyen, N. Ranganathan, and L. Yobas, "Experimental and computational analysis of droplet formation in a high-performance flow-focusing geometry," *Sens. Actuators A, Phys.*, vol. 138, no. 1, pp. 203–212, Jul. 2007, doi: 10.1016/J.SNA.2007.04.053.

[46] *Surface Tension Values of Some Common Test Liquids for Surface Energy Analysis.* Accessed: May 3, 2022. [Online]. Available: http://www.surface-tension.de/

KAISER PÄRNAMETS (Graduate Student Member, IEEE) was born in Tallinn, Estonia, in January 1989. He received the Bachelor of Science and Master of Science degrees in engineering from the Tallinn University of Technology, in 2013 and 2016, respectively, where he is currently pursuing the Ph.D. degree. From 2014 to 2017, he was a Hardware Engineer at the electronics industry. Since 2018, he has been an Electronics Lecturer for bachelor's and master's students. His research interests include lab-on-a-chip and microfluidics.

ANDRES UDAL (Member, IEEE) received the Ph.D. degree in electronic engineering from the Tallinn University of Technology, Tallinn, Estonia, in 1999. From 1990 to 1995, he was acting as a Visiting Researcher and a TCAD Software Designer at Silvaco Inc., Santa Clara, CA, USA; Darmstadt University of Technology, Germany; and Uppsala University, Sweden. He is currently a Senior Research Fellow with the Laboratory for Proactive Technologies, Department of Software Science, Tallinn University of Technology.

ANTS KOEL (Member, IEEE) was born in Tallinn, Estonia, in August 1962. He received the Engineer Diploma degree in industrial electronics from the Tallinn Polytechnic Institute, Estonia, in 1985, the master's degree, in 1998, and the Ph.D. degree from the Tallinn University of Technology, Tallinn, Estonia, in 2014. His research interests include semiconductor electronics and devices, TCAD simulations, and circuit design. He has been the Chairperson of the Steering Committee of the IEEE-Sponsored Baltic Electronics Conference, in 2020 and 2022, participated in ERA Chair projects COEL and 5GSOLAR, led electronics in-kind contribution projects of Estonia in European Spallation Source.

TAMÁS PARDY (Member, IEEE) received the M.Sc. degree in info-bionics engineering from Pázmáany Péter Catholic University, Budapest, Hungary, in 2014, and the Ph.D. degree in electronics and telecommunication from the Tallinn University of Technology, Tallinn, Estonia, in 2018. He is currently a Senior Researcher with the Tallinn University of Technology. He has supervised one Ph.D. thesis and three M.Sc. theses and has authored or coauthored 20 scientific publications. His research interests include flow- and temperature-control of lab-on-a-chip devices.

NAFISAT GYIMAH received the B.S. degree in electrical and electronic engineering from the Kwame Nkrumah University of Technology, Kumasi, Ghana, in 2013, and the M.S. degree in communicative electronics from the Tallinn University of Technology, Tallinn, Estonia, in 2020, where she is currently pursuing the Ph.D. degree in high-speed droplet microfluidics sorting and encapsulation. She was a Cognitronics Engineer at the Tallinn University of Technology, from June 2020 to December 2020. From November 2021 to January 2022, she worked at Selfdiagnostics Deutschland GmbH on the thermal and electrical characterization of SARS-CoV2 microfluidic multitest kits. Her research interests include lab-on-a-chip, droplet microfluidic system control, and flow control simulations using computational fluid dynamics (CFD).

TOOMAS RANG (Senior Member, IEEE) received the Ph.D. degree in semiconductor electronics from the Hungarian Academy of Sciences, in 1981. He is currently a Professor Emeritus with the Thomas Johann Seebeck Department of Electronics, and a Senior Research Fellow with the Department of Chemistry and Biotechnologies, Tallinn University of Technology, Estonia. His research activities related to research and development in the field of applied microfluidic approaches for lab-on-a-chip applications. He supervised 15 Ph.D. Students and fulfilled the PI position on several European and domestic research and industrial projects. He was the Initiator and an Honor Chairperson of the Baltic Electronics Conferences (BEC) series, in 1987, and has been supported by IEEE, since 1996.